Mechanical Behavior and Hardening Characteristics of a Superplastic Ti-6Al-4V Alloy

A. K. GHOSH AND C. H. HAMILTON

The deformation behavior of a superplastic Ti-6Al-4V alloy at 927°C has been characterized by means of constant strain-rate tensile tests up to large plastic strain. Significant hardening has been recorded in the course of deformation. Microstructural studies on deformed samples indicate the occurrence of simultaneous strain-rate induced grain growth, which explains nearly all of the hardening. A small amount of hardening may also be expected from grain elongation or grain clustering effects. As a result of concurrent grain growth, the strain-rate sensitivity is found to decrease with strain, thus indicating that stress-strain rate behavior determined initially may not be applicable after large amounts of plastic strain. The stress/strain-rate data obtained from step strain-rate test for a variety of grain sizes, together with the grain growth kinetics plots, provide a means for developing a constitutive description for this material at large strains.

THE superplastic properties of Ti-6Al-4V alloy above 900°C have now been demonstrated and fabrication of components using this technique is underway.[1] In the mill processed condition, the alloy typically has a fine grain size, ~5 to 7 μm, and at temperatures below the beta transus (*i.e.*, about 999°C), it contains a mixture of two phases: the more deformable β and the less deformable α. Presumably it is the presence of two phases that retards the grain growth in this alloy and permits a fair degree of superplasticity; for example, a maximum strain-rate sensitivity, $m = (d\ln\sigma/d\ln\dot{\epsilon})$, of about 0.85 at 927°C has been reported.[2,3] Large tensile elongations have also been observed, however, they are somewhat lower than what would be expected on the basis of their m values. Analytical prediction of elongation from m values have been found satisfactory for a number of materials,[4] and, therefore, the smaller observed elongations raise questions regarding the accuracy of plastic flow properties (σ-$\dot{\epsilon}$ data) of this material determined within the first few percent of deformation.

The primary intent of this work was to establish a fairly accurate characterization of the flow properties of this industrially important alloy for large plastic strain levels at 927°C. The interest stems obviously from the standpoint of application of such information in superplastic forming of components where large plastic strains are often encountered.

Several investigators have discussed the problems of measuring the σ-$\dot{\epsilon}$ behavior of a rate-sensitive material.[5,6] In step strain-rate tests in which $\dot{\epsilon}$ is suddenly incremented or decremented, the problem lies with the interpretation of the transient behavior. Load relaxation which appears to produce consistent results in a number of materials is also questionable since concurrent recovery at high temperatures can obscure the results. Additionally, relationship of this kind of measurement with forming characteristics (in which strain-rate in a deforming element continuously increases) has not been established yet.

Generally, superplastic materials are regarded as purely rate-sensitive, *i.e.*, no strain hardening occurring during deformation, for which stress is a unique function of plastic strain rate. Figure 1 shows the expected load-time behavior for such a material subjected to a constant total (elastic and plastic) strain-rate, $\dot{\epsilon}_t$. The plastic response is assumed to be given by $\sigma = K\dot{\epsilon}_p^m$, where σ = stress, $\dot{\epsilon}_p$ = plastic strain-rate, K = constant, m = strain-rate sensitivity index, and the elastic response given by $\sigma = E\epsilon_e$, where ϵ_e = elastic strain and E = elastic modulus. The values of the various parameters indicated on Fig. 1 are chosen such that they roughly represent Ti-6Al-4V at 927°C.

It is seen from Fig. 1 that considerable time passes before load maximum at a low applied strain-rate (10^{-4} s^{-1}). During this time, as shown in the upper graphs, elastic strain-rate drops from an initial value of 10^{-4} s^{-1} while plastic strain-rate begins to rise from zero. While $\dot{\epsilon}_p$ approaches $\dot{\epsilon}_t$ only asymptotically, it is reasonable to assume $\dot{\epsilon}_p = \dot{\epsilon}_t$ at load maximum, which is often utilized in the computation of m values. It is clear, however, that $\dot{\epsilon}_p$ is significantly lower than $\dot{\epsilon}_t$ during the rising part of the load curve on each point of which $\sigma = K\dot{\epsilon}_p^m$ is satisfied. It may, therefore, be difficult to infer such a material's plastic response from this portion of the curve without knowing the instantaneous plastic strain-rate. It appears that this is not commonly recognized, and in fact, the absence of sigmoidal shape in log σ-log $\dot{\epsilon}$ plots in Ref. 7 may be a result of selecting data from the rising part of the load curve.

Figure 1 also shows the expected load-time results for a higher applied strain-rate (10^{-3} s^{-1}). Shorter time to load maximum followed by a faster load drop are shown in this case, which is observed experimentally in these materials. In spite of a shorter time to load maximum, the strain to maximum load is greater at higher strain-rates, a fact often ignored during testing. The important point, however, is that stress and strain-rate at maximum load should reflect a nearly steady-state. The locus of these stress and strain-rate values from different constant $\dot{\epsilon}_t$ tests should then provide the flow properties for a superplastic material. Normally tests are conducted at constant crosshead speeds instead of constant

A. K. GHOSH and C. H. HAMILTON are with Science Center, Rockwell International, Thousand Oaks, CA 91360.

Manuscript submitted May 9, 1978.

ISSN 0360-2133/79/0611-0699$00.75/0

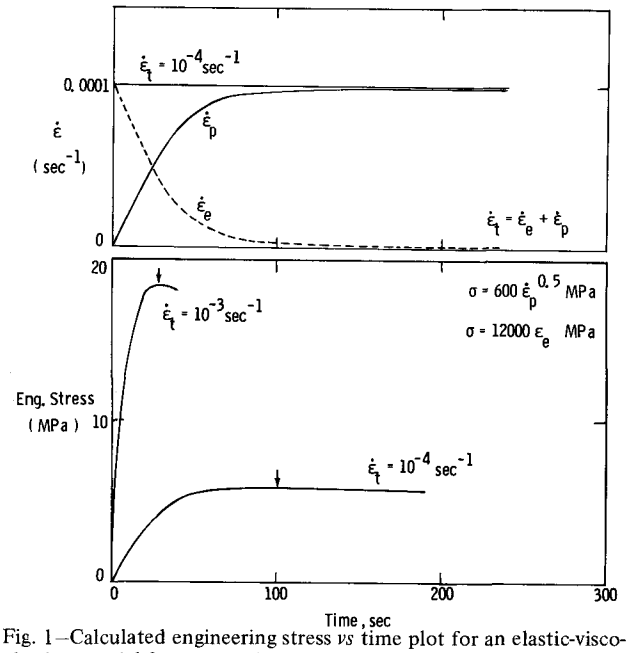

Fig. 1—Calculated engineering stress *vs* time plot for an elastic-visco-plastic material for two applied total strain rates. The constitutive equations are chosen to approximately represent Ti-6Al-4V at 927°C. The accompanying strain-rate *vs* time plot for $\dot{\epsilon}_t = 10^{-4}$/s shows initial elastic straining followed by gradual build-up of plastic strain.

strain-rates, and several such speeds are included in a single test by incrementing the speed (by 2/2.5 times) every time the load goes through a maximum. Specimen extension is assumed to be uniform which allows the use of crosshead displacement in the calculating of current strain-rate and current flow stress at each load maximum.

Figure 2 is a schematic load *vs* time plot during a step strain-rate test of Ti-6Al-4V at 927°C. The interesting features are that at the low crosshead speeds the load does not reach a maximum but continues to show a gradual rise, at some intermediate speed load reaches constant plateau, and at higher speeds it goes through a maximum and begins to show a sharp drop. The load rise at the low strain-rates,

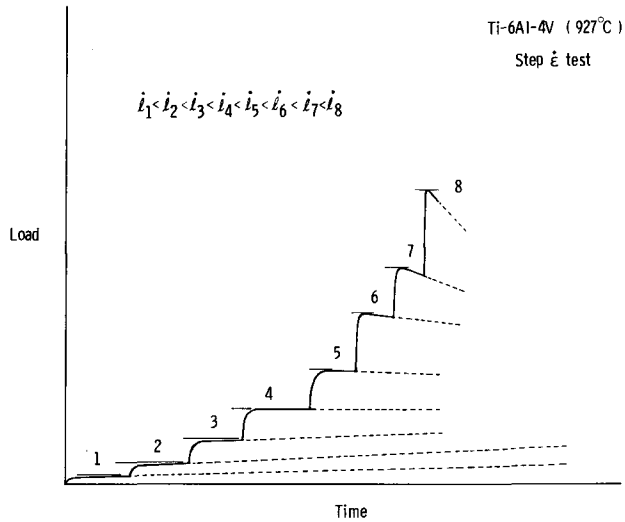

Fig. 2—Schematic plot of load *vs* time in tensile pulling of a superplastic material (*e.g.*, Ti-6Al-4V at 927°C) at progressively increasing crosshead velocities (step strain-rate test).

in spite of a slowdown in applied strain-rate, indicates hardening of the material with imposed strain. A part of this hardening is due to a rise in plastic strain-rate as shown in Fig. 1, which occurs very gradually when crosshead speed is low. However, the extent of hardening observed here is considerable and does not saturate even after significant plastic strain, which suggests other possible sources of hardening. This kind of hardening has been observed previously in other superplastic materials, such as Al-Cu eutectic[8,9] and is generally attributable to grain growth occurring during deformation. This is because a large contribution to deformation in these materials arises from their grain boundary regions, a reduction of which naturally leads to an increased resistance to flow. This possibility of concurrent grain growth during superplastic deformation which also suggests a continued change in the σ-$\dot{\epsilon}$ behavior prompted a closer look at this effect, particularly since the present interest lies in the behavior at large plastic strains. Suffice it to add that previous work[7-9] did not attempt this in any systematic manner. The following experimental program is therefore developed to meet this need.

In the course of this paper it will be found that the most significant improvement over past work[7] is the use of a constant true strain-rate test which avoids the excessive strain-rate drop during large superplastic extensions. Microstructural observations have also been correlated well with the deformation process by rapid quenching from the deformation temperature (not possible in Ref. 7). Furthermore, superplastic deformation is often assumed to be history-independent[7] thereby leading to errors in stress/strain-rate curves. On the other hand, systematic studies of static and dynamic grain growth have been conducted in our research program and related to the flow stresses. Another important input has been provided here by a technique of producing minuscule strain-rate increments, which do not perturb the structure appreciably and yield excellent rate-sensitivity indices. (This raises questions regarding the fixed value of 0.5 in Ref. 7.) Thus, considerable new insight into these and other areas of superplasticity has come out of this study.

EXPERIMENTAL

All tests were conducted on specimens taken from a single sheet (1.63 mm thick) of Ti-6Al-4V alloy.

Materials

Three starting grain sizes were utilized in the experimental program. These grain sizes were 6.4, 9.0, and 11.5 μm, respectively. While the first one represents the as-received material, the others were obtained by holding the as-received material at 955°C in vacuum for 2 and 7 h, respectively. Each of these reported grain sizes was actually measured from tensile specimens that were raised to the test temperatures of 927°C in the test fixtures, held for 10 min, and quenched, and, therefore, represent the grain sizes immediately prior to the tensile test. More about grain size will be said later.

Tensile Tests

In testing superplastic materials, constant crosshead speed generally leads to a decreasing strain-rate within the specimen gage length,* which additionally complicates the measurement of their mechanical behavior. An effort to maintain constant strain-rate included the following changes (see Fig. 3): 1) the specimen fillet region was reduced to a minimum to reduce its contribution to the overall extension, and 2) the crosshead speed was programmed to increase with specimen elongation so as to maintain a constant strain-rate (assuming the elongation to arise entirely out of the gage length). This latter function was performed by attaching a variable speed stepping motor to the drive gear of the Instron machine and using a programmable computer (Versatrak) to alter the input voltage to the motor in the following manner:

*At lower temperatures, when strain uniformity is not as great, the presence of fillets in the specimen can lead to an increasing strain-rate within the gage length even under a rising load.[10]

$$\text{voltage} \propto \text{crosshead speed} = l_o \dot{\epsilon}_t \exp(\dot{\epsilon}_t \tau)$$

where l_o = initial gage length, $\dot{\epsilon}_t$ = applied strain rate, τ = time from the start of test.

A five zone resistance furnace with 305 mm constant temperature zone was used for maintaining test temperature. To prevent oxidation, a static argon atmosphere with slight positive pressure was maintained by surrounding the specimen and pull rods in a long Inconel tube. Temperature during the test was held at 927 ± 2°C with less than a degree variation along the specimen length. The specimen heat-up time was nearly 90 min and a hold time of 10 min was allowed before each test. A total of four strain-rates was investigated. For two of these, 2×10^{-4} and 10^{-3}/s, three specimens were tested at each rate, and subsequently unloaded and quenched following true strain levels of 0.3, 0.66, and 1.0, respectively. For the other two strain-rates, 5×10^{-5} and 5×10^{-3}/s, one specimen was tested at each rate and was quenched after unloading. The quenching was performed by injecting argon gas directly on to the specimen at high velocity and was intended to "freeze" the high temperature microstructure. While water quenching would have been more desirable, it was avoided because of the associated difficulty. Due to the problem associated with quenching, the microstructures did exhibit variable morphology of the transformed β-structure. However, this poses no problem with the interpretation of high temperature structure containing undecomposed β-phase. In any event, a temperature drop of 600°C within 2 min was achieved by the argon quench which is so far one of the best for these tests.

A 2.54 mm diam circle grid pattern etched on the specimen prior to testing was utilized for strain measurements upon unloading. Figure 4 shows axial strain as a function of testing time for strain-rates of 2×10^{-4} and 10^{-3}/s. The variation within the gage length is indicated by the bars, while the open circles represent the specimen center. The desired constant strain-rate, indicated by the solid line, is seen to be followed well by the specimen. Even though the strain variation does increase with increasing strain-rate, the specimen center appears to deform very close to the desired rate. Areas selected for subsequent metal-

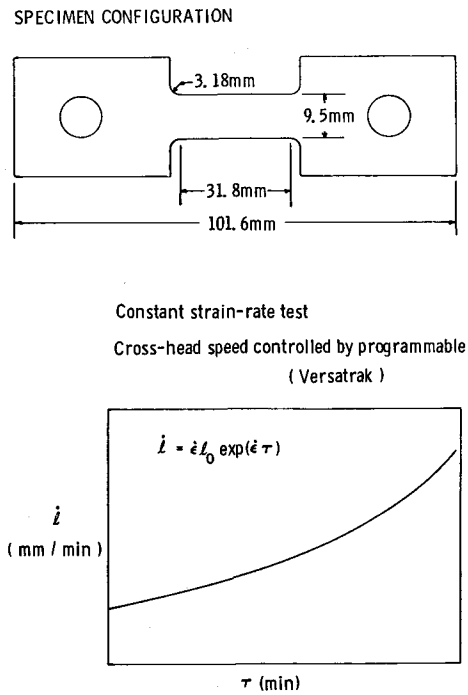

Fig. 3—Tensile specimen geometry with a minimum of fillet region and schematic representation for how crosshead speed was incremented as a function of time in order to maintain constant total strain-rate within the specimen.

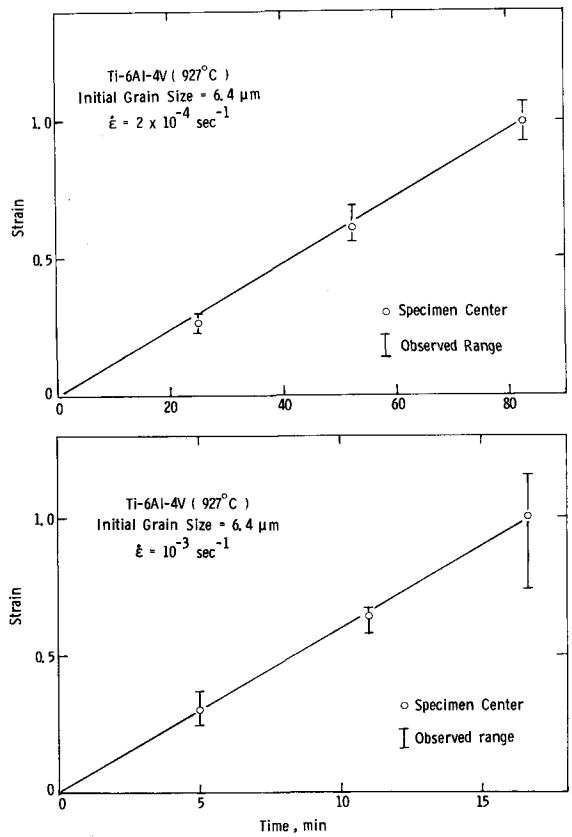

Fig. 4—Desired strain *vs* time plots in a tensile test (solid line) are compared with measured grid strains from specimens tested up to various strain levels. The bar indicates entire strain range in a specimen while the open circle represents specimen center.

lographic examination were also taken from specimen centers.

Although the material was found to be fairly isotropic with respect to superplastic properties, all tests were conducted in the transverse orientation in order to exclude the directionality variable.

The rolling planes (*i.e.*, planes parallel to the sheet surface) were examined for grain size in each specimen after quenching and strain measurement. In order to provide comparison with static grain growth behavior, specimens were held for different times (without deformation) at 927°C and water quenched. All grain size measurements in this work were carried out by three methods: 1) linear intercepts along the rolling direction, 2) linear intercepts along the transverse direction, and 3) Hilliard circle (20 cm). Both α- and β-grains are considered for grain size evaluation. Grain sizes reported are average grain diam, as determined by the following relation:[11] $1.68\ L/MN$, where N = number of intercepts, M = magnification and L = length of line. Grains are fairly equiaxed in the starting condition as well as after static grain growth. However, the deformed specimens do show grain elongation along the tensile axis. Bars on data points are used in the next section to incorporate this directional variation, the grain size from Hilliard circle lying within this range.

RESULTS AND DISCUSSIONS

During tensile tests at constant strain-rate, a continuous load rise was observed at the slower strain-rates and load drop at the higher strain-rates. Because of the high degree of strain uniformity here, it is reasonable to calculate instantaneous cross-section from axial strain assuming volume constancy and thereby compute the instantaneous flow stress even though the load drops. True stress-strain curves for all three initial grain sizes are shown in Fig. 5 for strain-rates of 2×10^{-4} and 10^{-3}/s while those for 6.4 μm material are also shown for 5×10^{-5} and 5×10^{-3}/s. The solid parts of the curves indicate extreme strain uniformity in the specimen while the finely dotted parts indicate the uncertainty due to increasing nonuniformity. A serrated stress-strain curve was shown for a strain-rate of 5×10^{-3}/s, perhaps indicating the occurrence of dynamic recrystallization. The shaded band envelopes the maxima and minima of such a curve.

All of these curves exhibit hardening of the material with increasing deformation. It appears that the extent of hardening with strain decreases with increasing strain-rate up to near 10^{-3}/s and then increases again for 5×10^{-3}/s. This is perhaps due to excessive strain hardening at the higher rate. The stress level is also found to increase with increasing grain size in agreement with previous findings.[3,7-9]

Microscopic examination of deformed and quenched specimens clearly indicated grain growth occurring during the test (similar to the observation by Lee and Backofen[3]) which might be responsible for the observed hardening. An initial grain size of 6.4 μm was found to grow on the average of 7.6, 8.4 and 8.9 μm following straining to 0.3, 0.6, and 1.0, respectively, at 10^{-3}/s which will be shown to be in excess of grain growth in absence of deformation. Measurable grain elongation has also been observed generally increasing with increasing strain and strain-rate.

Grain growth kinetics plots of Figs. 6 and 7 illustrate the average grain size *vs* time of exposure with and without concurrent deformation. Figure 6 is for an initial grain size of 6.4 μm at all the strain-rates under study. Figure 7 shows grain growth curves for strain-rates of 0, 2×10^{-4} and 10^{-3}/s for materials with initial grain sizes of 9 and 11.5 μm. The static grain growth curves in this figure are obtained from a master plot of static growth kinetics by reducing the total time of exposure by the amount of time required to reach 9 and 11.5 μm, respectively. It is clear from these plots that grain growth is enhanced by the imposed strain-rate and despite large scatter in the data the trend persists at all starting grain sizes. Limited data in Ref. 12 also suggested this possibility. Stress-assisted or strain-rate assisted grain boundary mobility has been observed before in

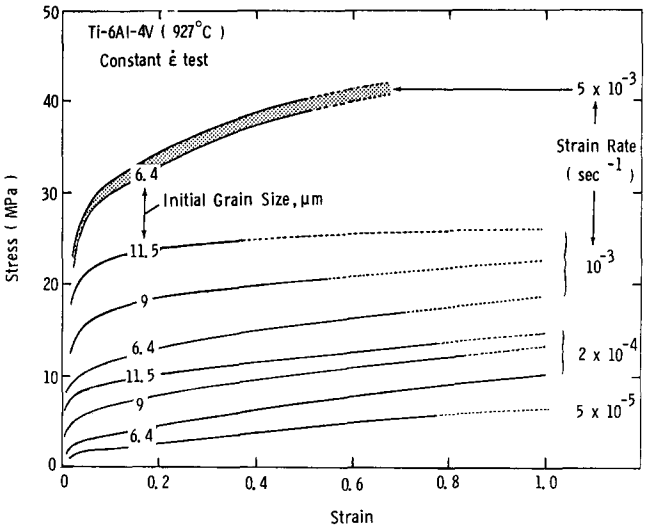

Fig. 5—True stress-strain curves for three initial grain sizes of 6.4, 9, and 11.5 μm, respectively. The bottommost curve shown is for a strain-rate of 5×10^{-5}/s, and the topmost one for 5×10^{-3}/s both for the 6.4 μm grain size material. The dotted part indicates significant strain gradient developing in the specimen.

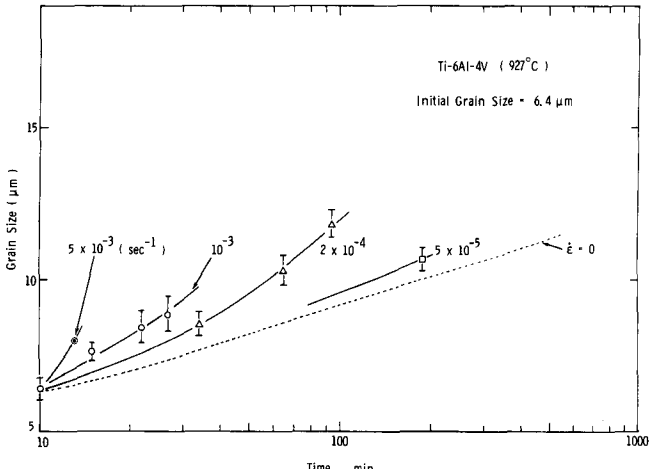

Fig. 6—Grain growth kinetics at four different tensile strain-rates compared with static kinetics for an initial grain size of 6.4 μm.

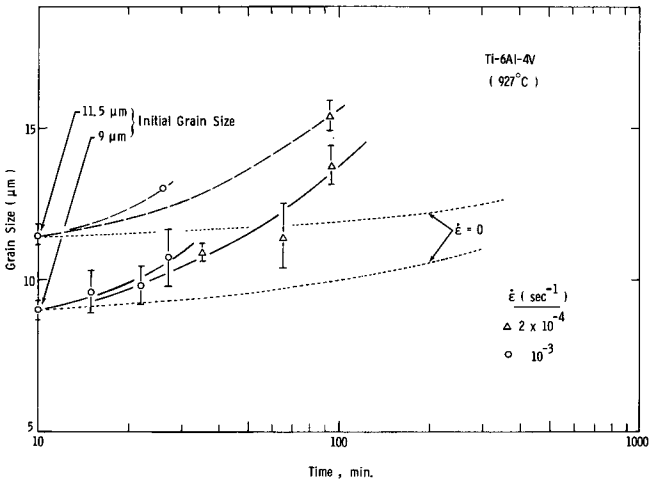

Fig. 7—Grain growth kinetics at two different tensile strain-rates compared with static kinetics for initial grain sizes 9.0 and 11.5 μm, respectively.

Pb (Ref. 13) and Cu-Al-Fe alloys[14] and relates to the enhanced grain growth observed in the present investigation.

For a unified view of the grain growth kinetics, the time scale in each plot of Fig. 7 is translated such that the initial grain size on these plots come to rest on the corresponding plots of Fig. 6 (*i.e.*, for the same strain-rate in each case). The resulting log (grain size) *vs* log (time) plots are shown in Fig. 8. The approximation to linear behavior in these plots is reasonable thus suggesting the relationship:

$$d = d_o\ (t/10)^n \qquad [1]$$

where d = current grain size, d_o = initial grain size, both in microns, t = time, in min, n is a parameter that increases with increasing strain-rate. An approximate value for this parameter for Ti-6Al-4V at 927°C is found to be:

$$n = 1.8\ (\dot{\epsilon}_t + 0.00005)^{0.237} \qquad [2]$$

where $\dot{\epsilon}_t$ has the dimension of s^{-1}. Equations [1] and [2] will be used subsequently in developing a constitutive equation for superplastic flow in this material.

With evidences of hardening as well as grain growth during deformation available, an attempt is now made

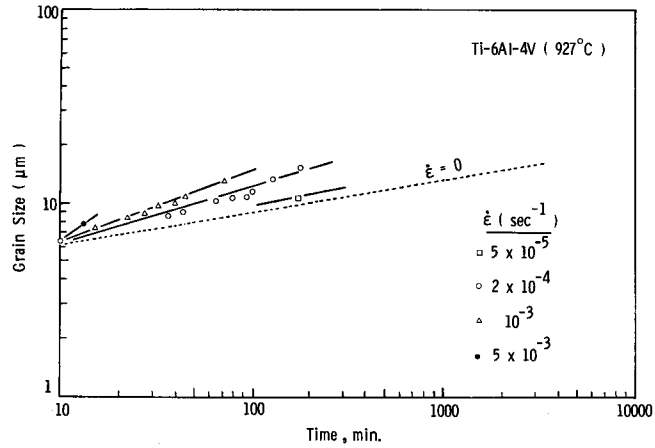

Fig. 8—Grain growth kinetics data from Figs. 6 and 7 have been reassembled in a log-log plot.

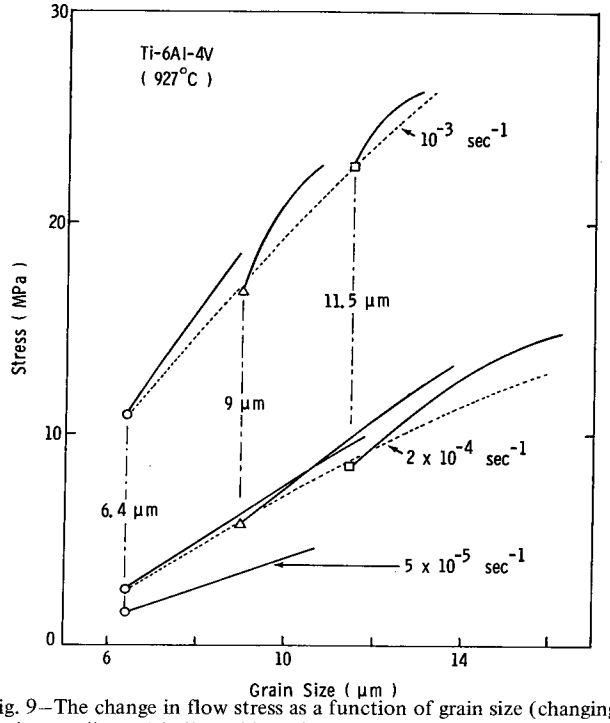

Fig. 9—The change in flow stress as a function of grain size (changing during tensile test) indicated by solid curves. The data points indicate the three initial grain sizes from which tests were started. The appropriate strain-rates are shown on the plot.

to relate the two in Fig. 9. This is done by cross-plotting flow stress from Fig. 5 against grain size during deformation, obtainable from the grain growth kinetics plots of Figs. 6 and 7 (for each applied strain-rate). The solid curves in Fig. 12 are thus grain growth hardening curves for initial grain sizes of 6.4, 9, and 11.5 μm for the various applied strain-rates. The flow stress corresponding to each initial grain size is indicated by a data point taken from the "knee" between the elastic and grossly plastic parts of the

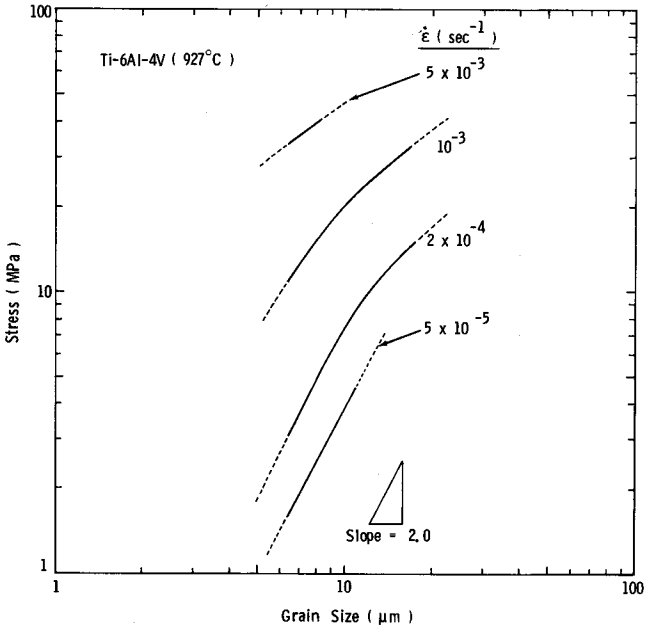

Fig. 10—Grain growth hardening curves at various strain-rates obtained by averaging each envelope of curves in Fig. 9.

load-extension plots and represents as much as 3 pct total strain. While there is some subjectivity in determining these points, the errors are no more than ±1 MPa.

The locus of initial flow stresses for each material, shown dotted, defines the basic, or initial, grain size dependence of flow stress for the indicated strain-rate. The solid curves rising above this indicate that deformation produces a small amount of hardening in excess of what might be expected from grain growth alone. This hardening may arise from the fact that grains do elongate in the course of deformation. On the basis of Ashby and Verral's grain switching model of superplastic flow,[15] the departure from equiaxed grain shape is expected to increase the resistance to boundary sliding. Even though their model was proposed for a single-phase material, this would intuitively appear to be true since the ease of grain boundary shear would be maximum when boundaries are at 45 deg to the tensile axis, which is more likely for an equiaxed grain structure.

Another possible reationale for the excess hardening might lie in the phenomenon of "grain clustering,"[16] whereby some of the neighboring like grains (*e.g.*, α-α or β-β) might behave as a unit rather than individual grains while participating in the grain switching mechanism. This may increase the "effective" grain size and, therefore, flow stress. Irrespective of the source, this hardening is a significantly smaller effect in comparison to the primary effect of grain growth hardening. If the excess hardening is ignored, however, the solid curves corresponding to each strain-rate are found to lie within a narrow band. Average curves that represent these bands are shown in Fig. 13 for all four strain-rates.

The grain size dependence of flow stress in Fig. 10 is found to change from $\sim d^2$ dependence for the lower strain-rates to less than $\sim d$ for the higher strain-rates. Intermediate strain-rates actually show a gradual changeover from the higher power to the lower dependence. The same is believed to hold for other strain-rates over a wider range of grain sizes than that investigated here. While these dependencies are larger than those observed by Lee and Backofen,[3] it is interesting to note that diffusional mechanisms of superplasticity do predict grain size dependencies of a similar order. For example, Nabarro Herring model[17,18] of through-the-grain diffusion predicts $\sigma \propto d^2$; Coble mechanism[19] of boundary diffusion predicts $\sigma \propto d^3$; Ashby-Verral's[15] diffusional accommodation of grain switching predicts $\sim(d^2 + d^3)$ dependence. Dislocation creep recovery mechanisms,[20] on the other hand, predict $\sigma \sim d^{1/2}$ and the changeover in slope observed in Fig. 13 is believed to relate to a change from a diffusional mechanism for lower strain-rates and/or smaller grain sizes to a dislocation creep mechanism for higher strain-rates and/or larger grain sizes.

The influence of grain growth on strain-rate sensitivity is illustrated in the next series of figures. The stress *vs* strain-rate plots in Fig. 11(*a*) are obtained from step strain-rate test in contrast to the constant

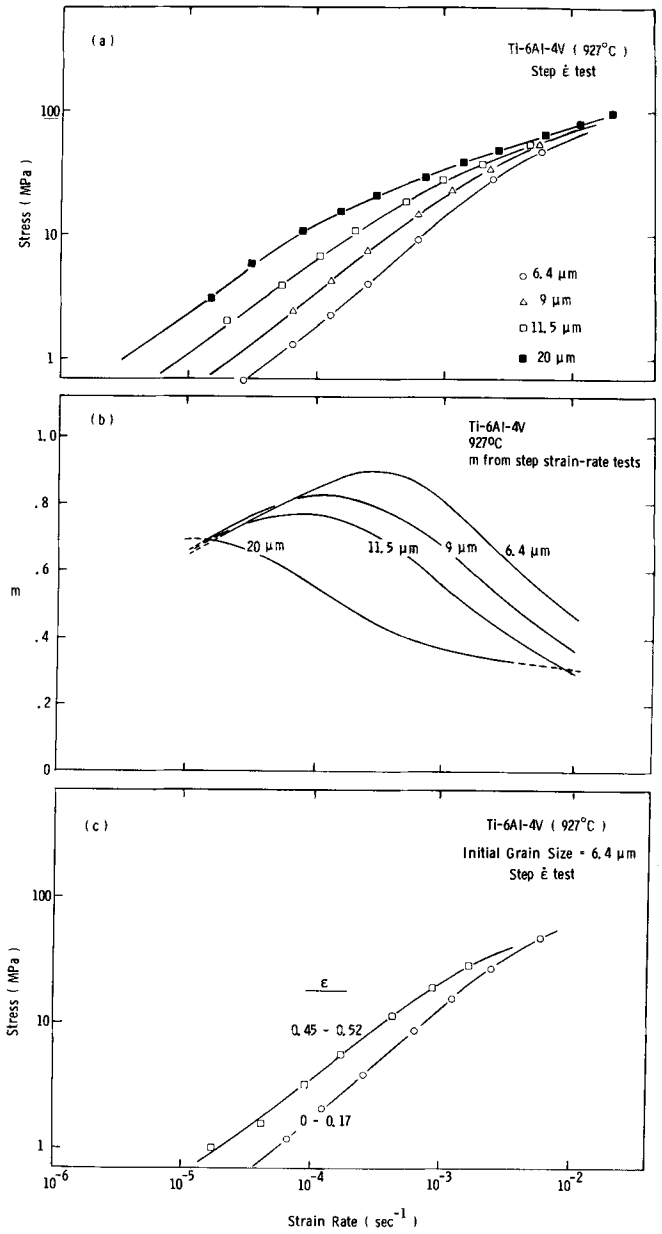

Fig. 11—(*a*) Stress *vs* strain-rate plots for four different initial grain sizes obtained by step strain-rate test. The data for 20 μm grain size material is from previous unpublished work, (*b*) Strain-rate sensitivity, *m*, given by the slopes of the curves in (*a*), (*c*) Stress *vs* strain-rate plots for 6.4 μm grain size material initially (*i.e.*, up to $\epsilon = 0.17$), and after a strain of 0.45 at a rate of 2×10^{-4}/s, showing hardening contribution due to the deformation exposure.

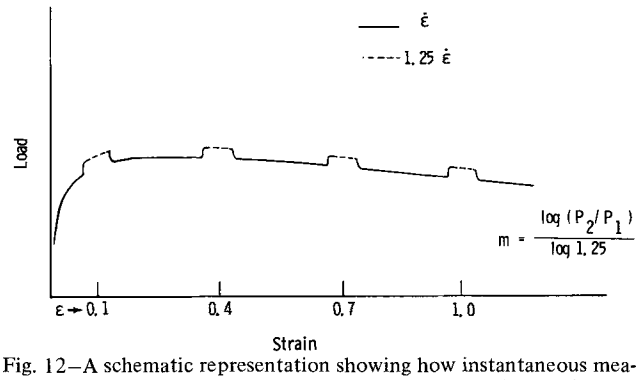

Fig. 12—A schematic representation showing how instantaneous measurements of *m* was made at periodic intervals during the tensile test, by strain-rate increments of 25 pct.

strain-rate test discussed so far. The test technique has been illustrated in Fig. 2, which does cause accumulation of strain as strain-rate is progressively stepped up. Hence the higher strain-rate portions of these plots contain some grain growth hardening. However, since the accumulated strain does not exceed 20 pct and its hardening contribution at the higher strain-rate is very small, the σ-$\dot{\epsilon}$ curves in Fig. 11(a) are considered to represent the three initial grain sizes fairly well. Results from a previous study[11] on a 20 μm grain size material is also included. While significant grain growth hardening is exhibited at the lower strain-rate, the curves approach each other at the high strain-rate end, thereby suggesting a drop in m ($= d \log \sigma / d \log \dot{\epsilon}$) with increasing grain size. Figure 11(b) shows m (*i.e.*, slope from Fig. 11(a)) as a function of $\dot{\epsilon}$ for the different grain sizes. These plots show a maximum in m at an intermediate strain-rate. The value of maximum m drops with increasing grain size as well as the strain-rate at which m_{max} is reached for each grain size. Data of this nature have been previously reported by Lee and Backofen.[3]

These results on different grain sizes compare well with those obtained from the same material after different amounts of strain. Figure 11(c) shows this in a material with initial grain size of 6.4 μm after deforming to a true strain of 0.45. While the initial test accumulated a strain of 0.17, subsequent deformation at 2×10^{-4}/s followed by step strain-rate test within the strain range of 0.45 to 0.52 clearly shows the hardening effect with associated drop in m.

The change in m with deformation is best studied in a constant strain-rate test, with periodic m determinations by strain-rate departures of small magnitude. This is schematically illustrated in Fig. 12, where the strain-rate was incremented by 25 pct only, maintained for 2 to 3 pct plastic strain and brought back to the original rate. (The controller was programmed to control these tests also.) It is felt that the small strain-rate departures did not alter the pattern of microstructural change that occurs at the original rate. The value of m here is determined from $m = \log (P_2/P_1)/\log (\dot{\epsilon}_2/\dot{\epsilon}_1)$, where P_2 is the load corresponding to a strain-rate of $\dot{\epsilon}_2$ and P_1 is the load at $\dot{\epsilon}_1$.

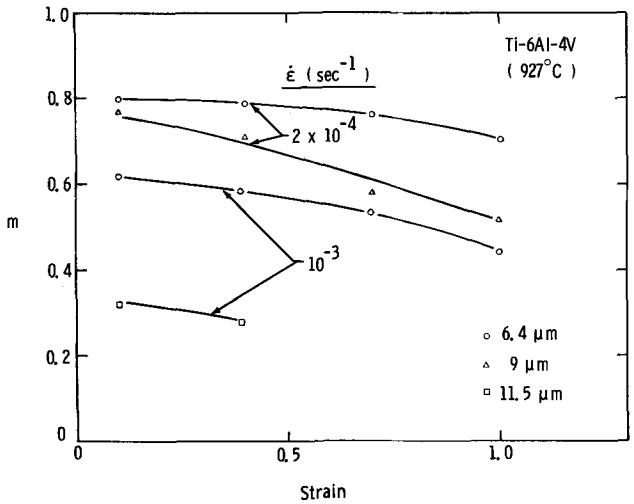

Fig. 13—Instantaneous values of strain-rate sensitivity during tensile test measured by the technique illustrated in Fig. 12, shows decreasing m with increasing strain.

These test results, shown in Fig. 13 for all three grain sizes, indicate that m decreases with strain. The values of m are found to be larger at the lower strain-rate and for the smaller grain size. The drop is more gradual for this case also. Coarser grains give rise to a lower m which also drops more rapidly with strain. During an actual forming operation, strain-rate in a deforming element changes continuously. However, it is this instantaneous value of m that determines its necking resistance at any instant. Thus m determined this way is perhaps the most meaningful parameter that can be related to ductility. It would, however, be a rather time consuming task to do this for a large number of strain-rate/grain size combinations in order to characterize the flow properties of such a material. Even if this is done, it is not clear how this information might be useful in plasticity modeling. It is, therefore, of interest to find a constitutive description for this material which incorporates the change in grain size. A further rationale for this is provided in the next figure.

It is a common practice[21] to describe high temperature mechanical behavior by plotting a family of log σ *vs* log $\dot{\epsilon}$ curves each at given strain level taken from

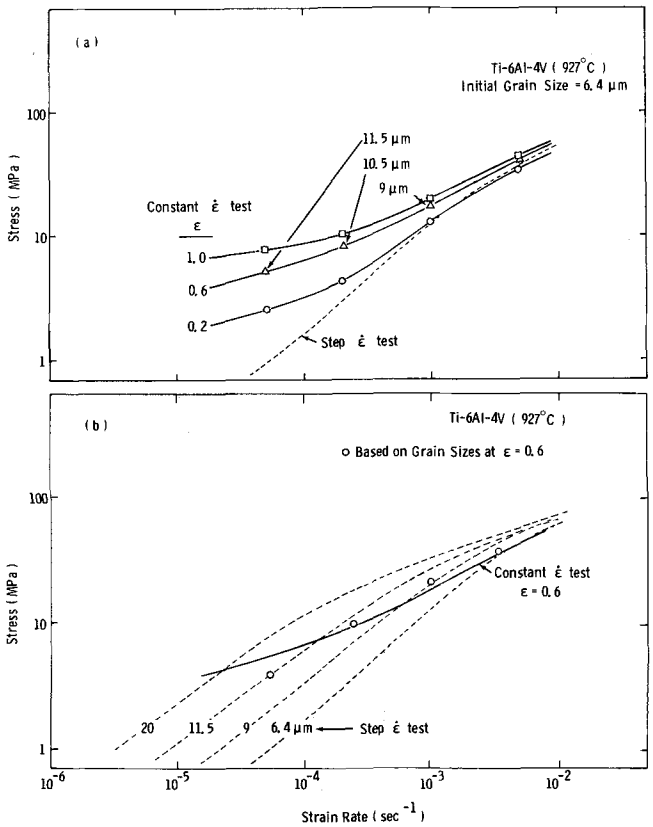

Fig. 14—(a) Flow stress from stress-strain curves of Fig. 5 are plotted as a function of strain-rate at fixed levels of strain. The initial grain size was 6.4 μm. Grain sizes attained at a strain of 0.6 (for different rates) are indicated on the plot, (b) The step strain-rate test data from Fig. 11(a) (dashed curves) are compared with the constant strain-rate data ($\epsilon = 0.6$) from Fig. 14(a) (solid curve). The family of dashed curves provides means of plotting any intermediate size by interpolation. This grid is used to show the approximate grain size/strain-rate combination expected from the grain growth kinetics plots of Fig. 6 for attaining a strain of 0.6 (open circles).

constant strain-rate test data. By taking slices at strain levels of 0.2, 0.6, and 1.0 in Fig. 5, and plotting the flow stress against corresponding strain rates in Fig. 14(*a*) we arrive at such a series of plots for an initial grain size of 6.4 μm. Also shown dotted is the σ-$\dot{\epsilon}$ data from step strain-rate test from Fig. 11(*a*). There is a significant difference between these curves particularly at the lower strain-rate obtained by the two different methods. This is because constant strain-rate test data incorporate grain growth hardening, the extent of which increases with decreasing strain-rate. Thus, at a strain of 0.2, the grain size for a test conducted at 5×10^{-5}/s is larger than that for a rate of 2×10^{-4}/s. This fact is also clear from the grain growth kinetics plots (Fig. 6), which show that while the rate of growth increases with strain-rate, the absolute grain size at a slower strain-rate is larger due to a longer time of exposure to reach that strain level.

Thus, along each solid curve in Fig. 14(*a*) a lowering of strain-rate amounts to a raising of grain size. This should correspond to a step strain-rate curve similar to the dotted curve but at a higher stress level (correspondingly larger grain size). Figure 14(*b*) illustrates this effect, in which the dotted curves are step strain-rate test data from Fig. 11(*a*). For a strain level of 0.6, the grain growth plots of Fig. 6 provide the appropriate grain sizes developed at different strain-rates. These grain size/strain-rate combinations are indicated (open circles) in Fig. 14(*b*) using the family of dotted curves as coordinate lines for interpolation. The solid curve is taken from Fig. 14(*a*) for $\epsilon = 0.6$ and agrees reasonably well with the open circle data. Thus, the rise in flow stress at the lower strain-rates yielding an obvious sigmoidal behavior is explainable. Given the step strain-rate data and grain growth kinetics, it is, therefore, possible to predict the results of a constant strain-rate test (or any arbitrary strain history) within experimental errors. This relationship between results obtained by the two different test methods also warns against determination of m from the plots of Fig. 14(*a*). It is clear that the slopes of these plots have no relationship to the strain-rate sensitivity of flow stress in a material whose microstructure changes during deformation.

SUMMARY

Constant strain-rate tests conducted on superplastic Ti-6Al-4V alloy at 927°C indicated concurrent grain growth. The grain growth rate is enhanced by imposed strain-rate, however, due to longer exposure times at lower strain-rates the absolute grain size for the same strain level becomes larger at the lower rates. Since flow stress of superplastic materials increases with increasing grain size, this concurrent grain growth during deformation leads to an apparent strain hardening. The flow stress has been found to change from a $\sim d^2$ dependence at the low rates to a $\sim d$ dependence at the higher strain-rates, where d = grain diameter. This suggests a diffusional mechanism of deformation at the lower rates and a power law creep mechanism at the higher rates.

The concurrent grain growth and associated hardening also lead to a drop in strain-rate sensitivity (m), thereby suggesting a poorer ductility than might be inferred from the initial value of m for this material. From a knowledge of grain growth kinetics (as a function of applied strain-rate) and basic stress *vs* strain-rate curve, it appears possible to construct a constitutive relation for this material for large plastic strains and arbitrary strain histories.

ACKNOWLEDGMENTS

The authors would like to thank Messers. L. F. Naverez and R. A. Spurling for experimental assistance.

REFERENCES

1. C. H. Hamilton: *Formability, Analysis, Modeling and Experimentation,* Proceedings of AIME Fall Meeting, Chicago, TMS-AIME Publication, 1978.
2. N. Paton: *J. Eng. Mater Technol.,* 1976, vol. 97, p. 313.
3. D. Lee and W. A. Backofen: *Trans. TMS-AIME,* 1967, vol. 239, pp. 1034-40.
4. A. K. Ghosh and R. A. Ayers: *Met. Trans. A,* 1976, vol. 7A, pp. 1589-91.
5. J. Hedworth and M. J. Stowell: *J. Mater. Sci.,* 1971, vol. 6, p. 1061.
6. C. P. Cutler: Ph.D. Thesis, University of Cambridge, 1971.
7. A. Arieli and A. Rosen: *Met. Trans. A,* 1977, vol. 8A, p. 1591.
8. B. M. Watts and M. J. Stowell: *J. Mater. Sci.,* 1971, vol. 6, pp. 228-37.
9. M. Surey and B. Baudelet: *J. Mater. Sci.,* 1973, vol. 8, pp. 363-69.
10. A. K. Ghosh: *Met. Trans. A,* 1977, vol. 8A, pp. 1221-31.
11. W. Rostoker and J. R. Drorak: *Interpretation of Metallographic Structures,* p. 224, Academic Press, 1976.
12. S. P. Agrawal, C. H. Hamilton, and E. D. Weisert: Unpublished research, Rockwell International Corporation, Los Angeles Division, 1977.
13. R. C. Gifkins: *Trans. TMS-AIME,* 1959, vol. 215, pp. 1015-22.
14. P. Ducheyne and P. DeMeester: *J. Mater. Sci.,* 1974, vol. 9, pp. 109-16.
15. M. F. Ashby and R. A. Verral: *Acta Met.,* 1973, vol. 21, p. 149.
16. D. J. Dingley: *Trends in Physics,* p. 319, European Physics Soc., Geneva, 1973.
17. F. R. N. Nabarro: *Report on Conf. on Strength of Solids,* p. 75, Phys. Soc., London, 1948.
18. C. Herring: *J. Appl. Phys.,* 1950, vol. 21, p. 437.
19. R. L. Coble: *J. Appl. Phys.,* 1963, vol. 34, p. 1679.
20. N. F. Mott: *Proc. Phys. Soc. B,* 1951, vol. 64, p. 729.
21. A. S. M. Eleiche: Air Force Report AFML-TR-72-125, Wright Patterson AFB, Dayton, OH, September 1972.